

See discussions, stats, and author profiles for this publication at: <https://www.researchgate.net/publication/23221017>

Influence of Plasticizer Type on the Properties of Polymer Electrolytes Based on Chitosan †

ARTICLE *in* THE JOURNAL OF PHYSICAL CHEMISTRY A · SEPTEMBER 2008

Impact Factor: 2.69 · DOI: 10.1021/jp801573h · Source: PubMed

CITATIONS

53

READS

141

4 AUTHORS, INCLUDING:



Agnieszka Pawlicka

University of São Paulo

153 PUBLICATIONS 1,458 CITATIONS

SEE PROFILE



E. Zygałło-Monikowska

Warsaw University of Technology

47 PUBLICATIONS 566 CITATIONS

SEE PROFILE

Influence of Plasticizer Type on the Properties of Polymer Electrolytes Based on Chitosan[†]Agnieszka Pawlicka,^{*,‡} Marins Danczuk,[‡] Wladystaw Wieczorek,[§] and Ewa Zygadło-Monikowska[§]

IQSC-USP, Av. Trabalhador São carlense 400, 13560-970 São Carlos-SP, Brazil, and Faculty of Chemistry, Warsaw University of Technology, ul. Noakowskiego 3, 00-664 Warsaw, Poland

Received: February 22, 2008; Revised Manuscript Received: May 27, 2008

Polymer electrolytes were obtained by the casting technique from a solution containing chitosan, hydrochloric acid, and plasticizer such as glycerol, ethylene glycol, and sorbitol. The transparent membranes with good ionic conductivity properties were characterized by impedance and UV–vis spectroscopies, thermal analysis (DSC), and X-ray diffraction. The best ionic conductivity values of $9.5 \times 10^{-4} \text{ S cm}^{-1}$ at room temperature and $2.5 \times 10^{-3} \text{ S cm}^{-1}$ at 80 °C were obtained for the sample containing 59 wt% of glycerol and an equimolar amount of HCl with respect to NH_2 groups in chitosan. The temperature dependence of the ionic conductivity exhibits an Arrhenius behavior with activation energy of 16.6 kJ mol^{-1} . The thermal analysis indicates that both glass transition temperature (-87°C) and crystallinity are low for this electrolyte. The samples with 13 wt% of LiCF_3SO_3 showed that the ionic conductivity values of $2.2 \times 10^{-5} \text{ S cm}^{-1}$ at room temperature and $4 \times 10^{-4} \text{ S cm}^{-1}$ at 80 °C are predominantly amorphous and showed a low glass transition temperature of about -73°C .

Introduction

Advances in display technology, batteries, and electrochromic devices have stimulated the study of solid polymeric electrolytes (SPEs). These kind of materials with lithium salts dissolved in a polymer matrix have been widely studied ever since the pioneering works of Wright et al.¹ and Armand et al.² These polymeric materials represent a promising alternative for the substitution of liquid electrolytes and inorganic crystals used in batteries, sensors, and electrochromic devices.^{3,4} Most of the systems described are composites and blends based on polyether chains that can be modified in order to decrease the crystallinity and glass transition temperature, improving the chain mobility and lithium ion conductivity. In addition, the world's trends toward scientific and technological progress in the area of new materials indicate the importance of using industrial and agricultural residues as raw materials. The utilization of these residues can minimize the problem connected with their accumulation and the use of traditional materials. Following these trends, electrolytes based on natural polymers such as starch,⁵ cellulose derivatives,⁶ chitosan,⁷ rubber,⁸ and gelatin⁹ are proposed. These polymers after physical and chemical modifications can be obtained in the transparent membrane form with very good adhesion properties to steel or glass. In addition, after the lithium salt addition, they can promote ionic conduction.

One of the most studied natural polymers is chitosan due to specific properties, such as biocompatibility and bioactivity, and also due to its promising potential in biomedical, pharmaceutical, and industrial applications.^{10,11} Chitosan also constitutes a polymer host for electrolytes because it is able to dissolve ionic salts^{7,12} and promote ionic conductivity.

The electrical properties of polymer electrolytes based on chitosan complexed with lithium and ammonium salts were recently reported.^{13–15} Conductivities on the order of $10^{-6} \text{ S cm}^{-1}$ at room temperature were reported for chitosan/poly(ethylene oxide) (PEO) blends with LiTFSI salt¹³ and for the complex formed by chitosan, poly(aminopropyl siloxane) (pAPS) and LiClO_4 .¹² Conductivities between 10^{-5} and $10^{-4} \text{ S cm}^{-1}$ were reported for polymer electrolytes based on swelling chitosan membranes and ammonium salts (NH_4NO_3 and $\text{NH}_4\text{CF}_3\text{SO}_3$), which in water promote the protonation of chitosan amino groups, leading to protonic conductivity.^{14,15}

Among different ionic conducting-polymer-based systems, those with plasticizers have attracted the attention of various research groups. An increase in ionic conductivity of 1–2 orders of magnitude and a decrease of T_g values by 40 °C of the plasticized polymeric samples were reported by MacFarlane et al.¹⁶ and Forsyth et al.¹⁷ In these works, the authors investigated the PEO samples plasticized with 50 wt% of propylene carbonate, 50 wt% of tetraglyme, and also 50 wt% of dimethyl formamide. Samples of plasticized chitosan-based polymer electrolytes were obtained by Arof et al.^{7,18,19} The authors showed that chitosan plasticized with 50 wt% of ethylene carbonate and the samples plasticized with 10 wt% of oleic acid showed the ionic conductivities of $10^{-5} \text{ S cm}^{-1}$. The authors of the present paper studied polymer electrolytes based on starch⁵ and hydroxylethyl cellulose^{6,20} plasticized with 30–48 wt% of glycerol and ethylene glycol, respectively. The best samples showed very good ambient temperature ionic conductivity of $10^{-3} \text{ S cm}^{-1}$.

In this work, new chitosan-based polymer electrolytes are presented. The samples of chitosan-based membranes containing HCl or HCl and LiCF_3SO_3 were plasticized with glycerol, ethylene glycol, or sorbitol, and the influence of these additives were correlated and compared with the samples containing LiClO_4 . The samples were characterized by structural (XRD), thermal (DSC), and spectral (impedance and UV–vis) measurements.

[†] Part of the special section for the "Symposium on Energetics and Dynamics of Molecules, Solids and Surfaces".

^{*} To whom correspondence should be addressed. E-mail: agnieszka@iqsc.usp.br. Tel.: (+55) 16 33739919. Fax: (+55) 16 33739952.

[‡] IQSC-USP.

[§] Warsaw University of Technology.

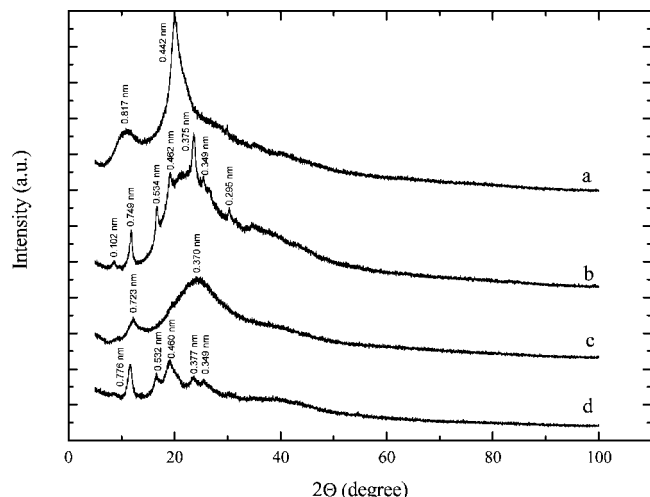


Figure 1. XRD pattern of chitosan-based samples; (a) chitosan powder, (b) chitosan-HCl (0.048 mol L⁻¹) membrane, (c) chitosan-HCl (0.048 mol L⁻¹) membrane plasticized with 59 wt% of glycerol, (d) chitosan-HCl (0.048 mol L⁻¹) membrane plasticized with 68 wt% of EG.

Experimental Section

The electrolytes were prepared according to the following procedure: 0.55 g of chitosan (Aldrich, No. 448877; average molecular mass of 3×10^4 – 6×10^4 ; viscosity of 200–800 cps with 1% CH₃COOH and measured deacetylation degree of 70%) was dispersed in 55 mL of hydrochloric acid solution in water (0.048 mol L⁻¹; equimolar amount to amine groups) under magnetic stirring for 12 h to complete dissolution. Then, the solution was filtered, and different quantities of plasticizer (glycerol, ethylene glycol (EG), or sorbitol) and, in some cases, lithium salt (LiCF₃SO₃) were added. This viscous solution was then poured on Petri plates and dried at 60 °C to form transparent membranes.²¹ The structure of the membrane was examined by X-ray diffraction measurements. The data were recorded using a Siemens D-5000 instrument with Cu K α radiation.

Differential scanning calorimetry measurements were obtained using Shimadzu DSC-50 equipment at a heating rate of 5 K min⁻¹ under a nitrogen atmosphere in the temperature range of 173–393 K.

The UV–vis optical spectra of the electrolytes were recorded with an Agilent spectrophotometer instrument between 200 and 1100 nm.

Impedance spectroscopy measurements were used to determine the ionic conductivity and frequency behavior of the electrolyte. A 2 cm round and 0.2 mm thick piece of the electrolyte was pressed against two steel electrodes. The measurements were taken with an Autolab instrument equipped with a FRA2 module, applying a voltage of 5 mV rms amplitude in the frequency range of $f = 10^6$ – 10^1 Hz.

Results and Discussion

XRD Analysis. Figure 1 shows X-ray diffraction patterns obtained for the chitosan and chitosan-based electrolytes having different compositions. The crystallization degree of 65% of chitosan was obtained from X-ray measurements (Figure 1a) using the following equation

$$X\% = (I_{\text{cr}} - I_{\text{am}}/I_{\text{cr}}) \times 100\% \quad (1)$$

where I_{cr} is the intensity of the crystalline diffraction peak at $2\theta = 20.1^\circ$ and I_{am} is the intensity of the amorphous broad

band centered at $2\theta = 10.9^\circ$.^{21,22} These results are similar to those presented by Nunthanid et al.²³ and by Drambei et al.,²² who obtained blends of chitosan with PVA.

The membranes obtained by casting from a solution of chitosan in hydrochloric acid show quite different diffractograms where more crystalline peaks with $d = 10.19$, 7.49, 5.34, 4.62, 3.75, 3.49, and 2.95 Å over a broad band centered around $2\theta = 22^\circ$ attributed to the amorphous state can be observed (Figure 1b). Clark and Smith²⁴ observed at least 18 peaks for the samples of HCl-modified chitosan. From these results, they obtained an orthorhombic structure with the parameters $a = 8.9$ Å, $b = 10.25$ Å, and $c = 17.0$ Å. They also did not exclude as an alternative the possibility of a monoclinic structure with $\beta = 88^\circ$. A comparison of our results of HCl-modified chitosan films with those of Clark and Smith's HCl-modified chitosan fibers from chitin (lobster carapace) results shows that four peaks are very similar, 4.46 (4.62), 3.56 (3.49), 5.13 (5.34), and 2.91 (2.95). However, due to the few peaks present, it is impossible to calculate the unit cell parameters. Further study by Ogawa and Inukai²⁵ of oriented fibers prepared from ungelled chitosan films yielded diffraction patterns indicative of high crystallinity, which were consistent with the monoclinic unit cell ($a = 13.8$, $b = 16.3$, and $c = 40.7$ Å and $\alpha = 96.48^\circ$) reported for chitosan salts (chloride, fluoride, and sulfate). By comparing the interplanar spacing of chitosan/HBr salt, 4.79 (4.62), 3.74 (3.75), 3.41 (3.49), that of chitosan/HI salt, 10.39 (10.19), 4.45 (4.62), 3.54 (3.49), 2.75 (2.95), and that of the very sharp pattern for chitosan/HCl samples of chitosan/HCl salt after annealing at 160° in an 80% isopropyl alcohol–water mixture, 7.87 (7.49), 5.53 (5.34), 10.69 (10.19), 3.43 (3.49), 3.75 (3.75), 4.60 (4.62), and 2.99 (2.95), it can be stated that our samples are similar to those obtained by Ogawa. The interpretation of these results can be explained following Cairns et al.,²⁶ who showed that *N*-, *N*,*O*-acetylated chitosan yields transparent gels which give high-quality fiber diffraction patterns indicative of high crystallinity and producing “chitin-like” junction zones within the gels. Moore and Roberts²⁷ proposed a model where they suggested that sufficient *N*-acetylation would overcome the electrostatic repulsion between protonated amine groups along the polysaccharide chain, leading to aggregation between chain segments as a result of intermolecular hydrogen bonding between *N*-acetylated regions.

The addition of glycerol to the membrane composition changes again the structural characteristics of the sample, and a very broad peak at $2\theta = 24.2^\circ$ and smaller one at $2\theta = 12.2^\circ$ are observed (Figure 1c), indicating an increase of the amorphous portion of the sample ($d = 7.23$ and 3.70 Å). Contrary to glycerol plasticized samples, the diffraction pattern of the samples plasticized with ethylene glycol (Figure 1d) showed five crystalline peaks at $2\theta = 11.4$, 16.7, 19.3, 23.6, and 25.5° ($d = 7.76$, 5.32, 4.60, 3.77, and 3.49 Å), which are almost the same as the samples of chitosan/HCl (7.87, 5.34, 4.62, 3.75, 3.49 Å). The difference is only in the width of the peaks, which can be explained by the presence of plasticizer, which promotes the distancing of the chains and changes of the crystalline structure. The difference in the crystallinity results between samples plasticized with glycerol and EG can be due to the more intense interaction between chitosan chains and EG, which is a smaller molecule than glycerol. These results are different when compared with the results of the ionic conducting samples based on chitosan plasticized with ethylene carbonate and reported by Arof et al.,¹⁹ who found all of the samples to be largely amorphous. However, some crystalline peaks can be observed in the XRD diffractograms of chitosan acetate

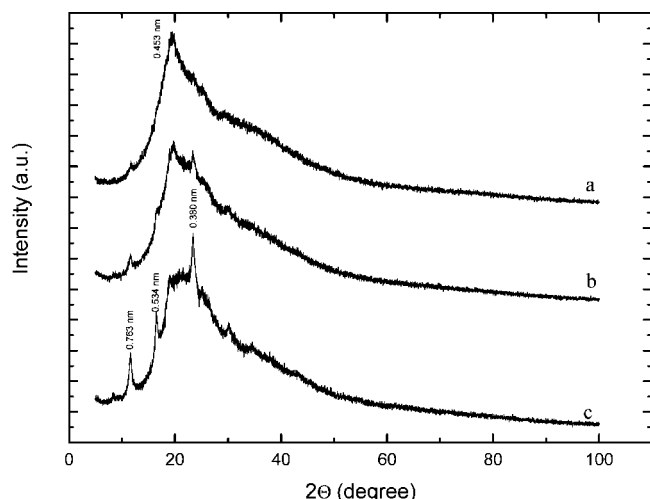


Figure 2. XRD pattern of chitosan–HCl (0.048 mol L^{−1}) based membrane samples plasticized with 48 wt% of glycerol and containing (a) 5, (b) 13, and (c) 33 wt% of LiCF₃SO₃.

plasticized with oleic acid samples.⁷ These differences can be due to the kind of plasticizer and its interaction with the natural polymer chain, where the long hydrocarbon chain of oleic acid can promote some local arrangement leading to the formation of crystalline regions. The formation of local arrangements is also observed in the case of samples plasticized with EG, where two-carbon molecules with hydroxyl groups on both sides can cross-link the chitosan chains through the hydrogen bonds.

Lertworasirikul et al.²⁸ showed that chitosan complexes show a wide variety of conformations, when compared with other polysaccharides. They suppose that it can be due to the regular distribution in the polymeric structure primary amino groups. These groups can form complexes with transition metals and salts from some acids. The conformation found for chitosan/HCl was a relaxed two-fold helical conformation having a tetrasaccharide as a helical asymmetric unit. As can be observed, the addition of plasticizer to the chitosan/HCl samples promotes a considerable increase of amorphous phase; however, in the case of addition of ethylene glycol as a plasticizer, the peaks are almost similar as those of the chitosan/HCl samples but larger due to the presence of plasticizer and very similar to the results presented by Belamine et al.²⁹ for the samples of chitosan extracted from shrimp shells and aged 5 h at 65 °C in hydrochloric acid.

Figure 2 shows the diffractograms of chitosan–HCl (0.048 mol L^{−1}) membranes plasticized with glycerol and containing different quantities of LiCF₃SO₃. As can be observed in this figure, the XRD pattern of the membrane samples changes with the addition of lithium salt. The diffractogram of the sample containing 5 wt% of the salt (Figure 2 a) is very similar to the results obtained for the chitosan powder (Figure 1a), where an accentuated peak is observed at $2\theta = 19.6^\circ$. The addition of the salt promotes an increase in the crystallinity of the samples evidenced, by the appearance of peaks at 11.6, 16.6, and 23.4° ($d = 7.63, 5.34$, and 3.80 \AA) for the sample with 33 wt% of salt (Figure 2c). Again, these results are different when compared with the samples of chitosan acetate plasticized with oleic acid and containing lithium acetate.⁷ It can be stated that the salt also promotes some local arrangement and creates crystalline regions.

Thermal Analysis. Thermal analysis by means of a differential scanning calorimeter (DSC) was performed in order to observe the change in the transition temperature caused by the change in the composition of the membranes samples. Table

TABLE 1: Glass Transition Temperature (T_g) and Ionic Conductivity Values for the Samples Obtained by Casting from a Solution with 0.048 mol L^{−1} HCl and Different Plasticizer (Glycerol and Ethylene Glycol (EG)) Contents

	plasticizer content (wt%)	T_g (°C)	conductivity (S cm ^{−1})
glycerol	0	−76	9.2×10^{-8}
	42	−82	7.5×10^{-7}
	59	−87	9.5×10^{-4}
	68	−83	1.8×10^{-4}
EG	42	−54	5.0×10^{-7}
	59	−59	6.0×10^{-6}
	68	−72	2.4×10^{-4}

TABLE 2: Glass Transition Temperature (T_g) and Ionic Conductivity Values for the Samples Obtained by Casting from Solution with Different HCl Concentrations and Containing 59 wt% of Glycerol

HCl concentration (mol L ^{−1})	HCl/NH ₂ –chit.	T_g (°C)	conductivity (S cm ^{−1})
0.032	0.77	−78	4.7×10^{-5}
0.048	1.00	−87	9.5×10^{-4}
0.065	1.57	−73	1.5×10^{-5}
0.114	2.75	−42	6.7×10^{-6}

TABLE 3: Glass Transition Temperature (T_g) and Ionic Conductivity Values for the Samples Obtained by Casting from 0.048 mol L^{−1} HCl, Containing 48 wt% of Glycerol and Different LiCF₃SO₃ Concentrations

LiCF ₃ SO ₃ (wt%)	T_g (°C)	conductivity (S cm ^{−1})
5	−56	1.7×10^{-5}
13	−73	2.9×10^{-5}
33	−50	3.5×10^{-6}

1 shows the influence of plasticizer, that is, glycerol and EG content, on the T_g and ionic conductivity values. It is possible to observe a decrease in the T_g with an increase of glycerol content up to 59 wt% and a continuous decrease of T_g for the samples with an increase of EG contents. Also, these quantities of plasticizer are much higher when compared with starch- and cellulose-based polymer electrolytes,⁵ which can be due to the more crystalline structure of chitosan. From these results, one can observe that the plasticized samples need more EG than glycerol to achieve almost the same values of the ionic conductivity. However, even with high plasticizer quantity and crystalline regions, samples plasticized with EG showed a low glass transition temperature and high ionic conductivity of $10^{-4} \text{ S cm}^{-1}$ at room temperature.

Table 2 shows the results of T_g obtained from thermal (DSC) analyses and ionic conductivity of the membrane samples containing 59 wt% of glycerol and different HCl concentrations. As can be stated in this set of results, a significant decrease of T_g and increase of one order of magnitude of ionic conductivity can be observed with an increase of acid concentration from 0.032 to 0.048 mol L^{−1}. After that, the increase of the acid concentration from 0.048 to 0.114 mol L^{−1} promotes an increase in the T_g and decrease of ionic conductivity of the samples. This can be due to the hydrolysis reactions of the chitosan polymeric chain leading to the destruction of the glycosides bonds. These reactions facilitate also the hydrogen-plasticizer interactions and ionic aggregate formation and, consequently, a decrease of ionic conductivity properties of the samples.

The samples containing lithium salt showed higher T_g values (Table 3) when compared with the samples without salt. Also, a significant decrease in T_g with increasing LiCF₃SO₃ concentration from 5 to 13 wt% and almost no difference in the ionic

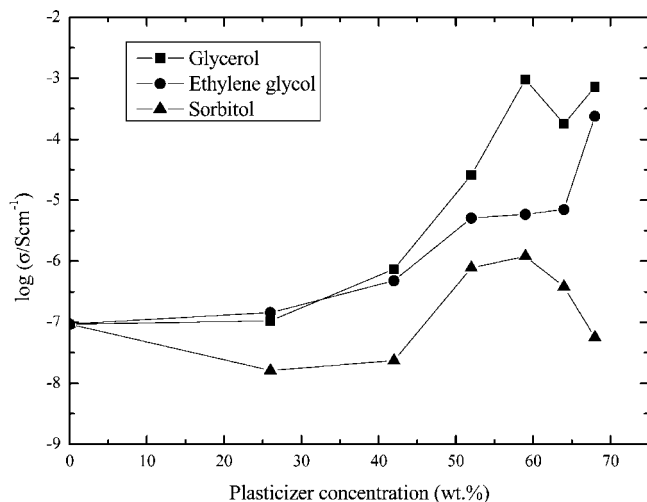


Figure 3. Log of ionic conductivity of the chitosan-HCl (0.048 mol L⁻¹) membranes as a function of glycerol (■), ethylene glycol (●), and sorbitol (▲) concentration.

conductivity values were observed. The higher quantity of salt (33 wt%) promotes an increase in the T_g and a decrease of the conductivity values of one order of magnitude. This increase in T_g may be attributed to the formation of ion pairs or ion clusters with an increase of the salt concentration, as already observed by Silva et al.³⁰ and Wiczeorek et al.³¹

Impedance Analysis. The membrane samples of chitosan-HCl with different concentrations of glycerol, EG, and sorbitol were subjected to ionic conductivity measurements, as shown in Figure 3. As observed in this figure, all samples show an increase in the conductivity values with increasing plasticizer concentration. However, samples with glycerol and sorbitol show a maximum of the conductivity values, and samples containing EG show an increase up to 68 wt%. For a higher concentration of EG, it was not possible to obtain the samples in the membrane form. The conductivity values of the samples increase from 9.2×10^{-8} (all samples without plasticizer) to 9.5×10^{-4} S cm⁻¹ for the sample with 59 wt% of glycerol and 2.4×10^{-4} S cm⁻¹ for the sample with 68 wt% of EG, that is, by four orders of magnitude. The lowest increase of the

conductivity values of the samples as a function of plasticizer contents was observed for sorbitol, where the best value was 1.2×10^{-6} S cm⁻¹ for 60 wt% of plasticizer. These conductivity values are comparable with those of 10^{-4} and 10^{-5} S cm⁻¹ obtained by Arof et al.^{7,18} and Ng et al.³² for the samples of chitosan plasticized with ethylene and propylene carbonate.

The differences in the conductivity values of samples can be due to the kind of plasticizer, its dielectric constant, viscosity, interaction with host polymer, and also molecular weight, where the plasticizer with lower molecular weight presents better plasticizer properties.^{33,34}

The ionic conductivity results as a function of temperature for the samples of chitosan-HCl (0.048 mol L⁻¹) containing different quantities of glycerol are shown in Figure 4. For all samples, a linear increase is observed in the conductivity values with temperature, which characterizes the ionic conduction mechanism as an Arrhenius one, that is, the hopping of conducting species, in this case, probably chloride (Cl⁻) ions between ammonium groups.³⁵ The same mechanism, however, more probably caused by lithium ions, is observed in the other plasticized SPE system, also starch-based electrolytes.⁵

As can be observed in Figure 4, the ionic conductivity values of the samples with glycerol increase with the plasticizer content up to 59 wt% and then decrease over the whole temperature range. Large quantities of the plasticizer lead to the system dilution and thereby to a decrease of the charge carrier concentration. The best conductivity results for chitosan-based membranes of 9.5×10^{-4} S cm⁻¹ at 30 °C and 2.5×10^{-3} S cm⁻¹ at 80 °C were obtained with the samples containing 59 wt% of glycerol.

In the case of the samples containing EG (Figure 5), a linear increase of the ionic conductivity values with temperature was also observed. However, as observed in Figure 3, three regions of conductivity are visible. The first one is for low EG concentration, the second one for the samples containing between 52 and 64 wt% of EG, and the third one for the sample with 68 wt% of EG. Also, the last one indicates the best conductivity values, which increase from 2.4×10^{-4} S cm⁻¹ at room temperature to 1.0×10^{-3} S cm⁻¹ at 80 °C. All of the samples showed the Arrhenius-type behavior.

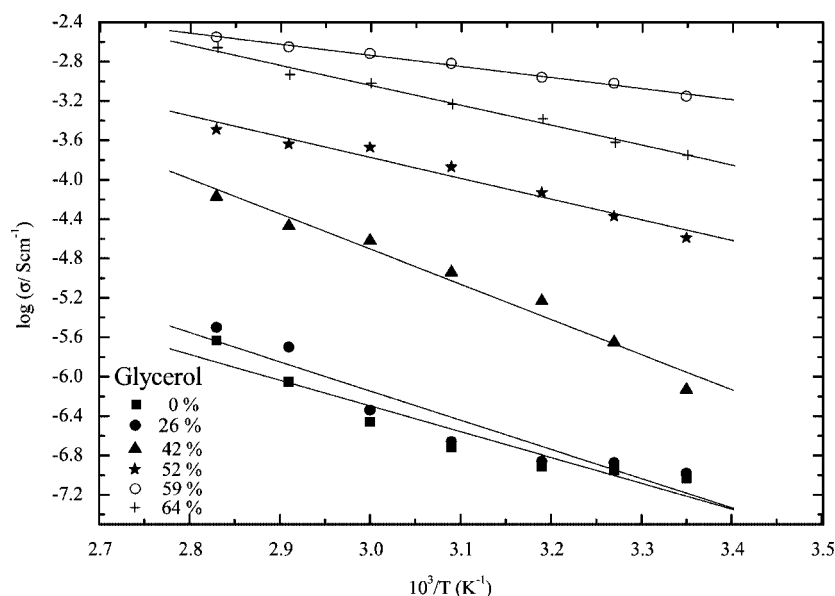


Figure 4. Arrhenius plots of the ionic conductivity of chitosan-HCl (0.048 mol L⁻¹) based membranes with different glycerol concentrations (0–64 wt%).

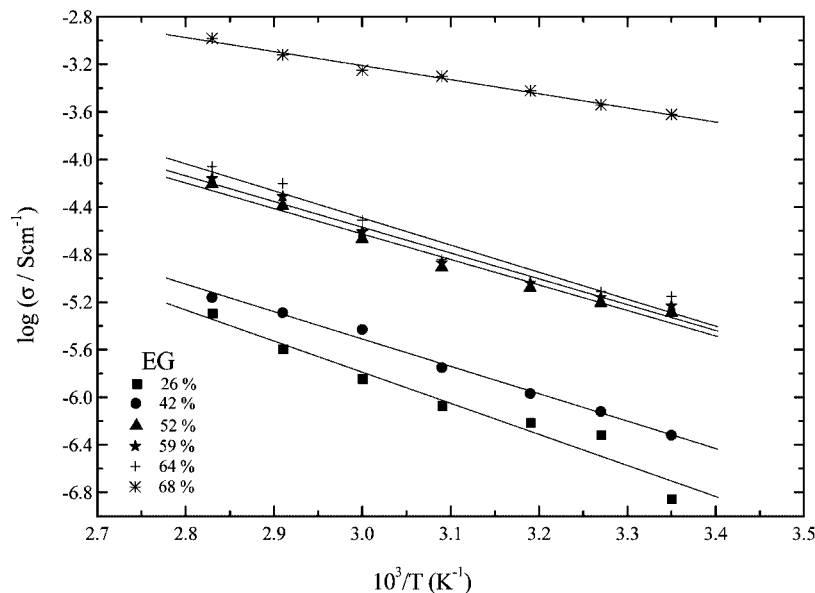


Figure 5. Arrhenius plots of the ionic conductivity of chitosan–HCl (0.048 mol L^{-1}) based membranes with different ethylene glycol concentrations (26–68 wt%).

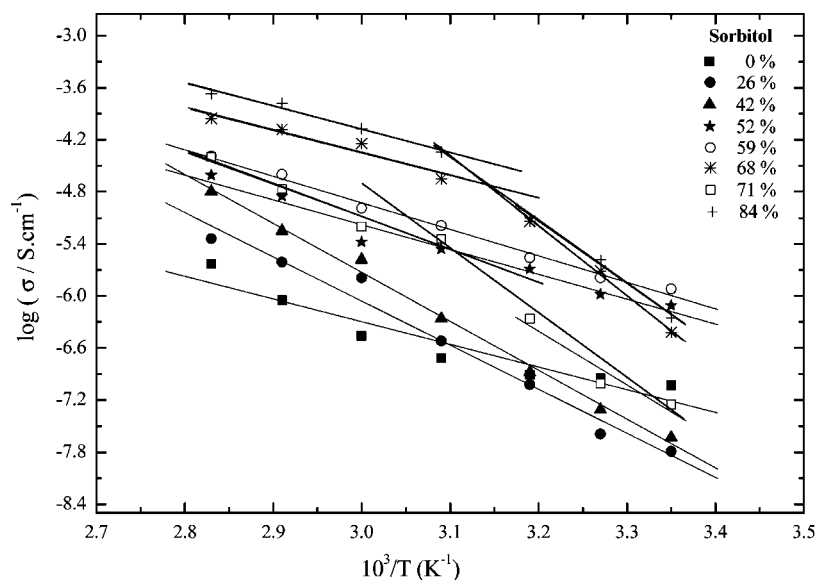


Figure 6. Arrhenius plots of the ionic conductivity of chitosan–HCl (0.048 mol L^{-1}) based membranes with different sorbitol concentrations (0–71 wt%).

The samples with sorbitol as the plasticizer (Figure 6) showed also a linear increase of the conductivity values with temperature, where the sample with 59 wt% of sorbitol showed the best results of $1.2 \times 10^{-6} \text{ S cm}^{-1}$ at room temperature and $4 \times 10^{-5} \text{ S cm}^{-1}$ at 80°C . From these measurements, it can be also stated that for higher plasticizer quantities, that is, more than 60 wt%, the Arrhenius plots can be adjusted with two linear fittings. A change of this linear fit slope changes from about 44°C for the sample with 68 wt% of sorbitol to 50°C for the sample with more than 70 wt%. It can be due to the increase of the crystalline phase in the samples with increasing plasticizer content.

For all of the samples, a linear increase of the conductivity with temperature was observed⁷ and can be explained by the Arrhenius model, where thermally stimulated charge carriers jump over the potential barriers from one site of complexation to another and generally in the direction of an electrical field promoting an electrical current. This is a model applied for the

whole polymeric volume and occurs in the non-organized polymeric structures. However, intermolecular, intramolecular, and interfacial movements, where the last one is the movement from amorphous to crystalline regions, can also be considered.^{36,37} Also, the interfacial movement is more probable in the chitosan-based system, where amorphous and crystalline phases are observed in the X-ray measurements (Figure 1).

From the measurement above, it was also possible to obtain the activation energies of the chitosan-based membranes. The samples plasticized with 59 wt% of glycerol showed $E_a = 16.6 \text{ kJ mol}^{-1}$, for the sample plasticized with 68 wt% of EG $E_a = 20.5 \text{ kJ mol}^{-1}$, and for the sample plasticized with 59 wt% of sorbitol $E_a = 37.3 \text{ kJ mol}^{-1}$.

Aiming to verify the influence of the concentration of HCl on ionic conductivity values of the chitosan-based samples of membranes plasticized with 59 wt% of glycerol, different concentrations of HCl were used, as shown in Figure 7. Usually, chitosan-based membranes contain acetic acid (weaker than

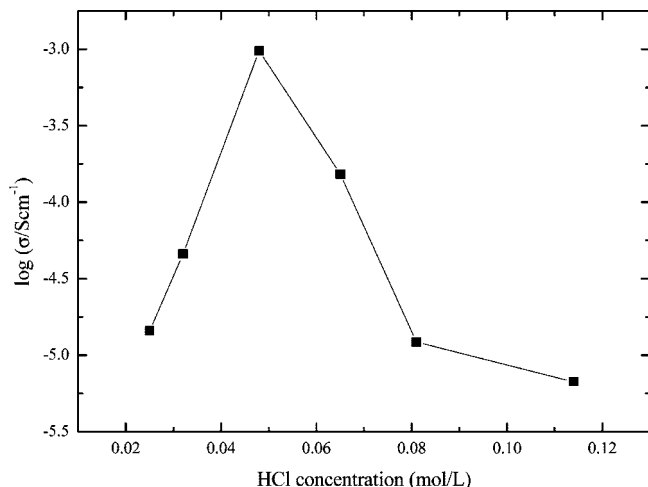


Figure 7. Log of ionic conductivity as a function of HCl concentration of the chitosan-based membranes plasticized with 59 wt% of glycerol, at room temperature.

HCl) and also lithium salts. The conductivity values reported by Arof et al.^{7,19} for this kind of samples are in the range of 10^{-5} S cm⁻¹ at room temperature. Yamada et al.³⁸ presented the results of anhydrous protonic chitosan samples with 200 wt% of methanediphosphonic acid and ionic conductivity values of 10^{-5} S cm⁻¹ at room temperature and 10^{-3} S cm⁻¹ at 150 °C. In the present work, the samples with 59 wt% of glycerol contained 0.025–0.114 mol L⁻¹ of HCl, that is, the ratio of HCl to NH₂ groups in chitosan were from 0.6 to 2.75. This experiment showed an increase of the ionic conductivity from 1.4×10^{-5} to 9.5×10^{-4} S cm⁻¹ for the samples containing 0.025–0.048 mol L⁻¹ of HCl. After that, an accentuated decrease of ionic conductivity values to 6.7×10^{-6} S cm⁻¹ for the samples containing 0.114 mol L⁻¹ of HCl was observed.

The addition of hydrochloric acid promotes the protonation of chitosan–NH₂ groups, which leads to the formation of polyelectrolyte chitosan–NH₃⁺ and consequently the ionic diffusion in the whole system. Also, protonation of water molecules and formation of H₃O⁺ and H₅O₂⁺ is possible, which can participate in the ionic conduction. The increase of the acid

concentration promotes an increase of the charge carriers and, consequently, the ionic conductivity up to a limit value. For higher than equimolar ratio (0.048 mol L⁻¹) acid concentration, the conductivity decreases, which is probably due to the formation of ionic pairs and aggregates of H⁺ with other ions and also hydroxyl groups of glycerol. An increase of the acid concentration promotes also the hydrolysis of the polysaccharide chain, increase of *T_g* values (Table 2), and increase in the crystallinity of the samples (data not shown here).

Again, all of the samples with different HCl concentrations showed a linear increase of the conductivity values with temperature (Figure 8), which can be explained by the Arrhenius model.

In order to verify the need to introduce the lithium salt and also its importance to the ionic conductivity of the system based on glycerol plasticized membranes and containing HCl, LiCF₃SO₃ was added. The ionic conductivity as a function of salt content is shown in Figure 9. In this figure, one can observe an increase in the conductivity values of 9.9×10^{-6} S cm⁻¹ for the sample without salt to 2.2×10^{-5} S cm⁻¹ for the sample containing 13 wt% of salt. This value is the maximum after which starts a decrease of the conductivity, reaching 3.5×10^{-6} S cm⁻¹ for the sample containing 33 wt% of salt. A decrease of conductivity is probably due to the chitosan and plasticizer competition for lithium ions³⁹ and interaction of CF₃SO₃⁻ anions with positively charged polymeric chain (chitosan–NH₃⁺), which promotes a rigid network formation.⁴⁰ These results are confirmed by the increase of *T_g* observed by thermal analysis (Table 3) and the increase of crystallinity, as shown in Figure 2.

The ionic conductivity values as a function of the temperature of samples containing a lithium salt showed also the Arrhenius-type dependence (Figure 10). In Figure 10, one can observe the increase in ionic conductivity from 1.1×10^{-5} S cm⁻¹ at room temperature to 1.9×10^{-4} S cm⁻¹ at 80 °C for the sample with 2.5 wt% of LiCF₃SO₃ and from 2.2×10^{-5} to 4×10^{-4} S cm⁻¹ in the same temperature range for the sample containing 13 wt% of salt.

Using these data, the energy activation values were obtained. It was observed that the activation energy for conduction decreased gradually with an increase in the LiCF₃SO₃ concen-

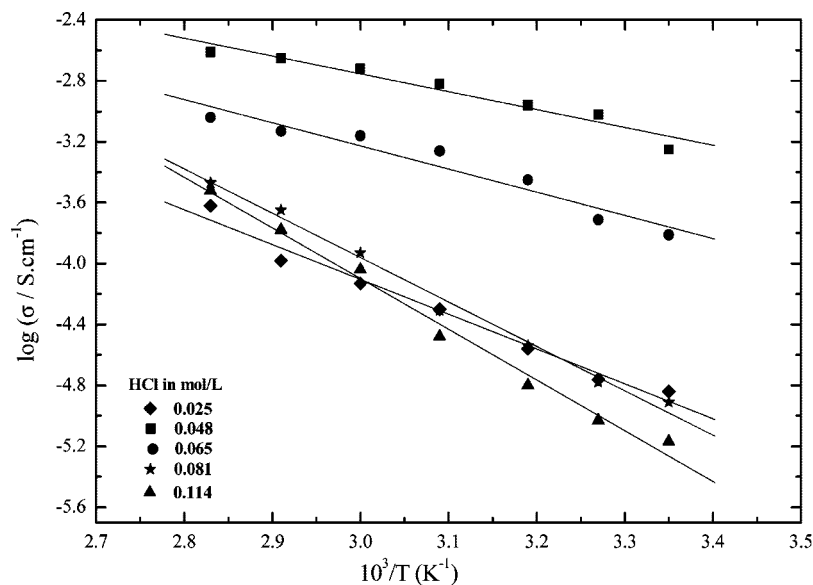


Figure 8. Arrhenius plots of the ionic conductivity of chitosan-based membranes containing 59 wt% of glycerol and different HCl concentrations.

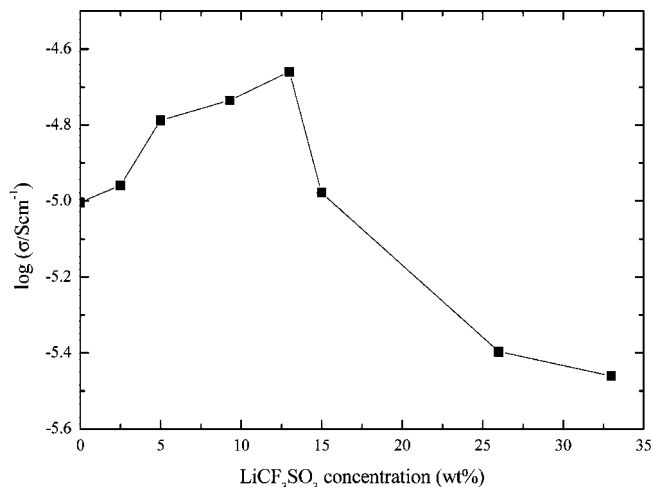


Figure 9. Log of ionic conductivity of chitosan-HCl (0.048 mol L^{-1}) based membranes plasticized with 48 wt% of glycerol and different LiCF_3SO_3 concentrations.

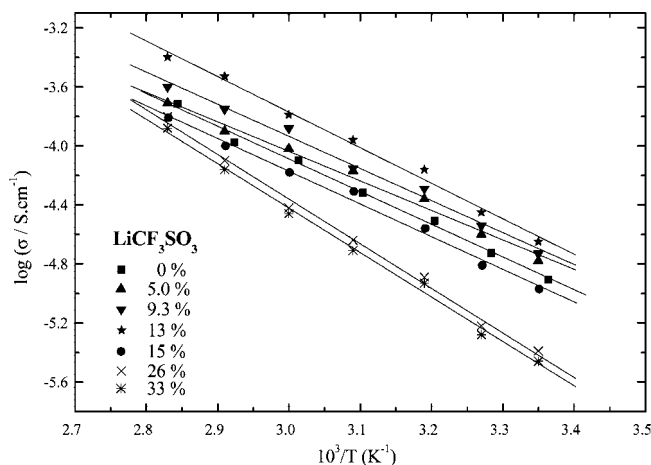


Figure 10. Arrhenius plots of the ionic conductivity of chitosan-HCl (0.048 mol L^{-1}) based membranes plasticized with 48 wt% of glycerol, containing different LiCF_3SO_3 concentrations.

tration up to 13 wt% of LiCF_3SO_3 , where the sample achieved the lowest $E_a = 27.7 \text{ kJ mol}^{-1}$. This is in agreement with the fact that the amount of ions in the polymer electrolyte increases by increasing the LiCF_3SO_3 concentration. Therefore, the energy barrier to the lithium transport decreases, which leads to a decrease in the activation energy.⁴¹ From this value, that is, 13 wt%, the activation energy starts to increase, that is, more energy is necessary for the movement of ions due to the closer distance between them.

The main/predominant mechanism of ionic conduction in these systems is also the Arrhenius-type model. However, the participation of polymeric chain movements in the ionic conduction is possible. This small contribution is due to the free volume of the polymer system increased by the plasticizer addition.⁴²

Optical Properties. Figure 11 shows the optical transmittance spectra for three different chitosan-based electrolytes in the 300–800 nm range. All of the samples showed very good transmittance in the visible region.

For the electrolyte containing acid and plasticizer, low transmission intensity can be observed below the 350 nm wavelength. Therefore, the transmission intensity starts to increase at 350 nm until it reaches 89–93% at 550 nm. The transmittance of the sample containing LiCF_3SO_3 is practically

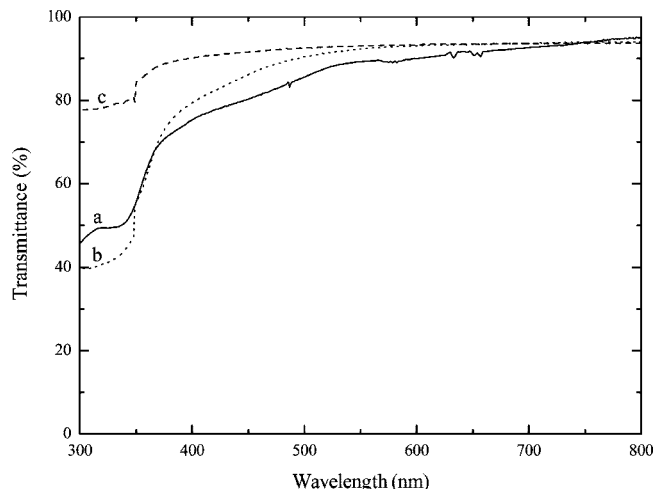


Figure 11. UV-vis transmittance spectra of chitosan-HCl (0.048 mol L^{-1}) based electrolytes containing (a) 59 wt% of glycerol, (b) 68 wt% of EG, and (c) 59 wt% of glycerol and 13 wt% of LiCF_3SO_3 .

constant over the whole visible range. This property makes the polymer electrolyte very attractive for use in electrochromic devices.

Conclusions

Polymer electrolytes based on plasticized chitosan and HCl or HCl and LiCF_3SO_3 salt were prepared. The samples were characterized by structural analysis (XRD), thermal analysis (DSC), and ionic conductivity as a function of additives and temperature and by spectroscopic measurements (UV-vis). It was observed that chitosan can be dissolved in HCl in different concentrations and plasticized with glycerol, ethylene glycol, and sorbitol, resulting in ion conductive samples. The best ionic conductivity values of $9.5 \times 10^{-4} \text{ S cm}^{-1}$ at room temperature and $2.5 \times 10^{-3} \text{ S cm}^{-1}$ at 80°C were obtained with samples containing an equimolar amount of HCl with respect to the amine groups (0.048 mol L^{-1}) and 59 wt% of glycerol. Samples containing LiCF_3SO_3 were also obtained and showed lower conductivity values when compared with the samples only with HCl. The best conductivity values of $2.2 \times 10^{-5} \text{ S cm}^{-1}$ at room temperature and $4 \times 10^{-4} \text{ S cm}^{-1}$ at 80°C were achieved with the sample containing 13 wt% of the lithium salt. The temperature dependence of the ionic conductivity of all of the samples exhibits an Arrhenius behavior with an activation energy of $E_a = 16.6 \text{ kJ mol}^{-1}$ for the sample plasticized with 59 wt% of glycerol, 20.5 kJ mol^{-1} for the sample plasticized with 68 wt% of EG, 37.3 kJ mol^{-1} for the sample plasticized with 59 wt% of sorbitol, and 27.7 kJ mol^{-1} for the sample with 13 wt% of LiCF_3SO_3 .

Thermal analysis and X-ray measurements indicate that both the glass transition temperature (-87°C) and crystallinity are low for the electrolyte with 59 wt% of glycerol and 0.048 mol L^{-1} of HCl.

All of the samples showed a high transmittance value of 89–93% at 550 nm. From these measurements, it can be stated that the polymer electrolytes based on chitosan, HCl, and glycerol are strong potential candidates for use in electrochromic devices.

Acknowledgment. The authors are indebted to FAPESP, CNPq, and the European Commission (Erasmus Mundus Program) for the financial support given to this research.

References and Notes

- (1) Wright, P. V. *Br. Polym. J.* **1975**, 7, 319.
- (2) Armand, M. B.; Chabagno, J. M.; Duclot, M. J. In *Fast Ion Transport in Solids*; Vashishta, P., Mundy, J. N., Shenoy, G. K., Eds.; North-Holland: Amsterdam, The Netherlands, 1979, p 131.
- (3) Vincent, C. A.; Scrosati, B. *Modern Batteries. An Introduction to Electrochemical Power Sources*, 2nd ed.; Arnold: London, 1997.
- (4) (a) Avellaneda, C. A. O.; Vieira, D. F.; Alkahlout, A.; Leite, E. R.; Pawlicka, A.; Aegerter, M. A. *Electrochim. Acta* **2007**, 53, 1648. (b) Alkahlout, A.; Pawlicka, A.; Aegerter, M. A. *Sol. Energy Mater. Sol. Cells* **2006**, 90, 3583.
- (5) Dragunski, D. C.; Pawlicka, A. *Mol. Cryst. Liq. Cryst.* **2002**, 374, 561.
- (6) Pawlicka, A.; Machado, G. O.; Guimarães, K. V.; Dragunski, D. C. *Proceedings of Spie* **2003**, 5136, 274.
- (7) Yahya, M. Z. A.; Arof, A. K. *Eur. Polym. J.* **2003**, 39, 897.
- (8) Glasse, M. D.; Idris, R.; Latham, R. J.; Linford, R. G.; Schlindwein, W. S. *Solid State Ionics* **2002**, 147, 289.
- (9) Vieira, D.; Avellaneda, C. O.; Pawlicka, A. *Electrochim. Acta* **2007**, 53, 1404.
- (10) Rinaudo, M. *Prog. Polym. Sci.* **2006**, 31, 603.
- (11) Muzzarelli, R. A. A.; Muzzarelli, C. *Adv. Polym. Sci.* **2005**, 186, 151.
- (12) Fuentes, S.; Retuert, J.; Gonzalez, G. *Electrochim. Acta* **2003**, 48, 2015.
- (13) Idris, N. H.; Majid, S. R.; Khiar, A. S. A.; Hassan, M. F.; Arof, A. K. *Ionics* **2005**, 11, 375.
- (14) Majid, S. R.; Arof, A. K. *Physica B* **2005**, 355, 78.
- (15) Khiar, A. S. A.; Puteh, P.; Arof, A. K. *Physica B* **2006**, 373, 23.
- (16) MacFarlane, D. R.; Sun, J.; Meakin, P.; Fasouloupoulos, P.; Hey, J.; Forsyth, M. *Electrochim. Acta* **1995**, 40, 2131.
- (17) Forsyth, M.; Meakin, P. M.; MacFarlane, D. R. *Electrochim. Acta* **1995**, 40, 2339.
- (18) Arof, A. K.; Osman, Z.; Mornin, N. M.; Kamarulzaman, N.; Ibrahim, Z. A.; Muhamad, M. R. *J. Mater. Sci.* **2001**, 36, 791.
- (19) Osman, Z.; Ibrahim, Z. A.; Arof, A. K. *Carbohydr. Polym.* **2001**, 44, 167.
- (20) Machado, G. O.; Ferreira, H. C. A.; Pawlicka, A. *Electrochim. Acta* **2005**, 50, 3827.
- (21) Wan, Y.; Creber, K. A. M.; Peppley, B.; Bui, V. T. *Polymer* **2003**, 44, 1057.
- (22) Drambei, P.; Nakano, Y.; Bin, Y.; Okuno, T.; Matsuo, M. *Macromol. Symp.* **2006**, 242, 146.
- (23) Nunthanid, J.; Puttipipatkachorn, S.; Yamamoto, K.; Peck, G. E. *Drug Dev. Ind. Pharm.* **2001**, 27, 143.
- (24) Clark, G.; Smith, A. F. *J. Phys. Chem.* **1936**, 40, 863.
- (25) Ogawa, K.; Inukai, S. *Carbohydr. Res.* **1987**, 160, 425.
- (26) Cairns, P.; Miles, M. J.; Morris, V. J.; Ridout, M. J.; Brownsey, G. J.; Winter, W. T. *Carbohydr. Res.* **1992**, 235, 23.
- (27) Moore, G. K.; Roberts, G. A. F. *Int. J. Biol. Macromol.* **1980**, 2, 78.
- (28) Lertworasirikul, A.; Noguchi, K.; Ogawa, K.; Okuyama, K. *Carbohydr. Res.* **2004**, 339, 835.
- (29) Belamine, E.; Dormard, A.; Giraud-Guille, M.-M. *J. Polym. Sci., Part A: Polym. Chem.* **1997**, 35, 3181.
- (30) Silva, M. M.; Barros, S. C.; Smith, M. J.; MacCallum, J. R. *Electrochim. Acta* **2004**, 49, 1887.
- (31) Wieczorek, W.; Lipka, P.; Zukowska, Z.; Wycislik, H. *J. Phys. Chem. B* **1998**, 102, 6968.
- (32) Ng, L. S.; Mohamad, A. A. *J. Power Sources* **2006**, 163, 382.
- (33) Sobral, P. J. A.; Monterrey-Q, E. S.; Habitante, A. M. Q. B. *J. Therm. Anal. Calorim.* **2002**, 67, 499.
- (34) Thomazine, M. T.; Carvalho, R. A.; Sobral, P. J. A. *J. Food Sci.* **2005**, 70, E173.
- (35) Urugami, T.; Yoshida, F.; Sugihara, M. *Macromol. Rapid Commun.* **1983**, 4, 99.
- (36) Nagashima, H. N.; Deaecto, G. S.; Malmonge, I. F. *Rev. Matér.* **2004**, 9, 445.
- (37) Golodnitsky, D.; Ardel, G.; Peled, E. *Solid State Ionics* **2002**, 147, 141.
- (38) Yamada, M.; Honma, I. *Electrochim. Acta* **2005**, 50, 2837.
- (39) Donoso, J. P.; Lopes, L. V. S.; Pawlicka, A.; Fuentes, S.; Retuert, P. J.; Gonzalez, G. *Electrochim. Acta* **2007**, 53, 1455.
- (40) Ward, I. M.; Boden, N.; Cruickshank, J.; Leng, S. A. *Electrochim. Acta* **1995**, 40, 2071.
- (41) Kopitzke, R. W.; Linkous, C. A.; Anderson, H. R.; Nelson, G. L. *J. Electrochem. Soc.* **2000**, 147, 1677.
- (42) Cha, E. H.; MacFarlane, D. R.; Forsyth, M.; Lee, C. W. *Electrochim. Acta* **2004**, 50, 335.

JP801573H